Tanzania Journal of Science and Technology
ISSN 2507-783X(print) and eISSN 2591-6742(electronic)
Journal homepage: https://journals.out.ac.tz/index.php/tjst

The Capability of Artificial Neural Networks as a Model for Predicting Total Electron Content (TEC): A Review

Emmanuel D. Sulungu
Department of Physics, College of Natural and Mathematical Sciences,
The University of Dodoma, Dodoma, Tanzania.
Email: edsulungu@gmail.com

Abstract
The results of investigations from a complete analysis of ANN application on Total Electron Content (TEC) prediction are presented in this paper. TEC is important in defining the ionosphere and has many everyday applications, for example, satellite navigation, time delay and range error corrections for single frequency Global Positioning System (GPS) satellite signal receivers. The total electron content (TEC) in the ionosphere has been measured using GPS. GPS are not installed in every point on the earth to make global TEC measurements possible. As a result, it is crucial to have certain models that can aid to get data from places where there is not any in order to comprehend the global behavior of TEC. Neural Network (NN) models have been shown to accurately anticipate data patterns, including TEC. The capacity of neural networks to represent both linear and nonlinear relationships directly from the data being modeled is what makes them so powerful. The survey from literature reveals that, Levenberg-Marquardt algorithm is preferred and used mostly because of its speed and efficiency during learning process, and that ANN showed a good prediction of TEC compared to the IRI model. As a result, NNs are suitable for forecasting GPS TEC values at various locations if the model's input parameters are well specified.

Keywords: *Artificial neural network; Global positioning system; Total electron content*

INTRODUCTION

The sun, which provides energy for life on Earth but also causes space weather, has an impact on the Earth's atmosphere (Chauhan *et al*., 2011; Leong *et al*., 2011; Oron *et al*., 2013; Okoh *et al*., 2019). Space weather refers to any and all states and events caused by the Sun in near-Earth space and the upper atmosphere, which can disrupt space-borne and ground-based technological systems (Kataoka and Pulkkinen, 2008; Wik *et al*., 2009; Shenvi and Virani, 2023; Li and Wu, 2023), and which can have an impact on human existence (Hanslmeier, 2002). Users of equipment such as televisions, radios, and computers, as well as anyone who uses Global Positioning System (GPS) in any manner, are affected by space weather (Sulungu *et al*., 2018b). In addition, space weather has an impact on all passengers flying in jet aircraft in high-latitude zones in both hemispheres (Hanslmeier, 2002). Induced electrical currents in long undersea communications cables, long-haul telecommunication lines, and certain fiber-optic systems are among the other disruptions caused by space weather phenomena (Wik *et al*., 2009).

Disturbances in the systems indicated above are due to changes in the concentrations of charged particles at different ionospheric heights induced by solar influences (Hanslmeier, 2002; Adolfs and Hoque, 2021; Ozkan, 2022), which alter the reflection, absorption, or transmission of electromagnetic waves through it. The ionosphere is the part of the atmosphere that is ionized, containing free electrons and positive ions (Kelley, 2009; Smirnov *et al*., 2023). The quantity of positively charged ions and negatively charged electrons is normally equal, resulting in an electrically neutral medium (Memarzadeh, 2009). During the ionization process, free electrons and ions are produced by the interaction of Extreme Ultraviolet (EUV) and X-ray radiations with the upper atmospheric neutral gas. The number of electrons and ions in the ionosphere is maintained by a continuous process of gaining and losing between their rate of production, which is controlled by the intensity of solar radiation and incident particles, and the rate at which newly freed electrons and ions recombine to produce reconstructed neutral particles (Eddy, 2009). Because of the free electrons, the ionosphere is an inhomogeneous propagation medium for electromagnetic waves, altering satellite signal transmission by modifying their velocity and direction of travel. The impact of the ionosphere, according to Norsuzila *et al*., (2010a) is that it can generate range-rate inaccuracies for GPS satellite users that require high accuracy data. The severity of ionospheric impacts is determined by a variety of factors, including the user's location, the time of day, the season, the status of the earth's geomagnetic field, and the level of solar activity (Leong *et al*., 2011).

A variety of instruments, including the GPS, have been used in studies to better understand the physical and chemical processes that occur in the ionosphere and plasmasphere (GPS) (Chen *et al*., 2022). The GPS's main purpose is to provide users with global navigation, positioning, and time information (Norsuzila, 2010a; Sulungu *et*

al., 2018b). However, the GPS is currently being used to provide data on the Total Electron Content (TEC) of the ionosphere (Liu *et al*., 2013). TEC is important for defining the ionosphere and has a variety of practical uses, including satellite navigation, delay time, and range error corrections for single frequency GPS (Bhuyan and Borah, 2007; Guoyan *et al*., 2021; Sulungu *et al*., 218b; Xiong *et al*., 2021).

The TEC is the total number of electrons integrated along the path from a terrestrial or spacecraft receiver to each GPS satellite and is measured in TECUs, where 1TECU = 1 x 10^{16} electrons/m^2 (Chauhan *et al*., 2011; Guoyan *et al*., 2021; Lee *et al*., 2021; Norsuzila *et al*., 2010b; Tang *et al*., 2022). It serves as a measure of ionospheric variability. The TEC is given by;

$$TEC = \int_{S_1}^{S_2} N_e dS \qquad (1)$$

where N_e denotes the ionospheric electron density and S the signal propagation path length between satellite and receiver positions S_2 and S_1, respectively.

The ionosphere causes a transmission time delay in electromagnetic waves that pass through it. The TEC and the frequency of electromagnetic waves are connected to the magnitude of this effect (Gao and Liu, 2002). According to Hunt *et al*. (2000), the temporal delay generated on a radio frequency signal travelling between S_1 and S_2 can be calculated as follows:

$$\Delta t = \frac{e^2}{8\pi c m_e \varepsilon f^2} \int_{S_1}^{S_2} N_e dS = \frac{40.3}{cf^2} TEC \qquad (2)$$

where c represents the speed of light in vacuum, m_e represents the electron mass, e represents the charge of an electron, f represents the transmitted frequency, and ε is the permittivity constant. In meters, the ionospheric range delay (phase advance) is given as:

$$\Delta R = c\Delta t \qquad (3)$$

where ΔR is the amount that would be added to the range if the range was calculated under the assumption that the radio signal travels at the speed of light. From (2) and (3) we get the following:

$$\Delta R = \frac{40.3}{f^2} TEC \qquad (4)$$

A dual-frequency GPS receiver measures the difference in ionospheric delay between the two signals, L1 and L2 with frequencies f_1 *and* f_2, which are obtained from the fundamental frequency, f_o = 10.23 MHz, so that:

$f_1 = 154 f_o = 1575.42$ MHz and

$f_2 = 120 f_o = 1227.60$ MHz

For a dual-frequency GPS receiver, the group delay is given as:

$$P_2 - P_1 = 40.3 TEC \left(\frac{1}{f_2^2} - \frac{1}{f_1^2} \right) \qquad (5)$$

P_1 and P_2 are pseudo ranges visible on L1 and L2 transmissions, respectively, and f_1 and f_2 are the corresponding high and low GPS frequencies.

To get the TEC, equation (5) can be written as follows (Sulungu *et al*., 2018b; Sulungu and Uiso, 2019):

$$TEC = \frac{1}{40.3} \left(\frac{f_1^2 f_2^2}{f_1^2 - f_2^2} \right) (P_2 - P_1) \qquad (6)$$

TEC is divided into two types: slant TEC (TECs) and vertical TEC (TECv). Because different GPS satellites are viewed at arbitrary elevation angles, TECs is a measure of the total electron content of the

ionosphere along the ray path from the satellite to the receiver measured at differing elevation angles. To compare the electron contents of pathways with various elevation angles, the TECs are converted into comparable TECv by assuming that the ionosphere is compressed into a thin shell with a shell height h, as shown in Figure 1.

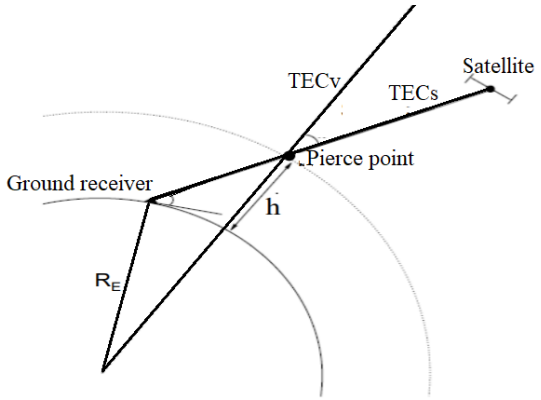

Figure 1: Ionospheric thin shell (Shim, 2009)

At altitude h, the TECv are allocated to an ionospheric pierce point (IPP), which is the intersection of the line-of-sight ray and the thin shell. TECv is frequently calculated from TECs using the following mapping function (Shim, 2009):

$$TECv = M(e) \times TECs, \tag{7}$$

where $$M(e) = \left[1 - \left(\frac{\cos(e)}{1 + h/R_E}\right)^2\right]^{\frac{1}{2}} \tag{8}$$

Here, e represents a satellite's elevation angle, h represents the height of the ionospheric shell, and R_E represents the Earth's mean radius.

However, GPS receivers are not installed at every location on the earth to allow global TEC measurements. As a result, it is essential to have some models that can help gather data from regions with no receiver in order to comprehend the TEC's global behavior (Sulungu and Uiso, 2019). The International Reference Ionosphere (IRI) is a globally utilized empirical ionospheric model for TEC forecasting. However, in places where data is poor, the IRI model does not provide accurate forecasts (Akir *et al*., 2015; Watthanasangmechai *et al*., 2012). As a result, models based on Neural Networks (NN) are used to forecast TEC (Sivavaraprasad *et al*., 2020). Neural Networks (NNs) are commonly employed in predictive modeling because of their learning and pattern recognition capabilities. They have been shown to be powerful tools that can learn trends and patterns in specific data and, as a result, accurately predict future trends and patterns for that data (Adolfs and Hoque, 2021). It has also been demonstrated that by altering the weights, a neural network may be trained to execute a certain purpose (Demuth and Beale, 2002; Okoh *et al*., 2016). The capacity of neural networks to capture both linear and nonlinear relationships directly from the data being modeled is one of its most powerful features (Okoh *et al*., 2016).

Therefore, the results from a comprehensive application of Artificial Neural Network (ANN) on TEC prediction are presented in this study. In comparison to other models such as the International Reference Ionosphere, the applicability of ANN in predicting TEC is discussed. The study also highlighted a number of authors' perspectives on the use of ANN in TEC prediction.

Ionospheric Modeling

Several models have been created over the last several decades to better understand the physics that affects the dynamics of the ionosphere. Empirical models are one of the sorts of models that have been developed; they provide an average ionosphere behavior based on observable data. However, the amount of data and the spatial and temporal coverage of the data that are employed in their construction limit these models (Shim, 2009). Despite these limitations, empirical models are extensively utilized due to their simplicity (Sulungu *et al*., 2018a). The NeQuick model (Nigussie *et al*., 2012) and the International Reference Ionosphere (IRI) model (Bilitza, 1986) are two examples of such models.

The IRI model

The International Reference Ionosphere (IRI) was established by the Committee on Space Research (COSPAR) and the International Union of Radio Science (URSI) in an effort to create an international standard for the specification of ionospheric parameters based on all available data from both ground-based and satellite observations from around the world (Kenpankho *et al*., 2011). The model is based on experimental evidence gathered from all available ground and space data (Bilitza *et al*., 2014). As new data and modeling methodologies become available, the IRI model is regularly upgraded (Sulungu *et al*., 2018a), resulting in many major editions of IRI.

There are three topside options that the IRI model employs to predict TEC, these are the NeQuick option, the IRI-2001-corrected option, and the IRI-2001 option. The NeQuick option is the default option for the IRI model in its standard form (Leitinger *et al*., 2001; Rathore *et al*., 2015). The inputs of the IRI model are latitude and longitude, date and time in UT, and altitudes ranging from 60 to 2000 km. The IRI model, on the other hand, has a lot of outputs, such as electron density, electron temperature, ion composition, ion temperature, F2-layer peak height, density, and TEC (Kumar *et al*., 2015). The IRI model's accuracy in a specific location is determined by the availability of trustworthy and plentiful data in that area (Adewale *et al*., 2011). For example, because of the vast number of stations in the northern mid-latitude region, the model could make accurate predictions there (Bilitza and Reinisch, 2008).

Artificial Neural Network (ANN)

ANN is made up of several simple processing units (layers) that communicate with each other by transmitting signals via a large number of weighted connections (Unnikrishnan *et al*., 2018). Each layer takes input from its neighbors or external sources and uses it to create an output signal that is transferred to the next layer. The neural system is made up of three layers: an input layer that receives data from outside the neural network, a hidden layer that keeps the input and output signals within the neural network, and an output layer that sends data out of the neural network (Anderson, 1997; Galushkin, 2007; Kröse and van der Smagt, 1996).

Topologies of Neural Networks

Feed-forward networks and recurrent networks are two types of neural networks

that differ in their layer connections and data propagation patterns.

Layers in feed-forward networks are connected in one direction to allow data to flow from the input to the output layer and do not allow closed paths inside the network connections; examples include Perceptron and Adaline (Haykin, 2001). In a feed-back connection, some or all layers have connections that allow them to move backwards to the preceding layer (Habarulema, 2010; Kröse and van der Smagt, 1996) (Figure 2).

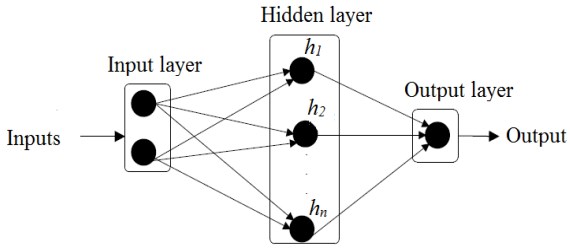

Figure 2: Three layers of a feed forward network (Habarulema, 2010)

On the other hand, in recurrent networks, there are no feedback connections. The network's dynamical features are crucial in this type of network. In some circumstances, the activation values of the units go through a relaxation process, resulting in the network reaching a stable state where the activation values do not vary. In some applications, the change in the activation values of the output neurons is significant enough that the network's output is determined by its dynamical behavior (Kröse and van der Smagt, 1996; Pearlmutter, 1990). These include the Elman network (Figure 3) which feeds some of the hidden unit activation values back to the input layer, to a group of extra neurons known as the context units, and the Jordan network that feeds output values back to the input layer, to a set of extra neurons known as the state units (Figure 4).

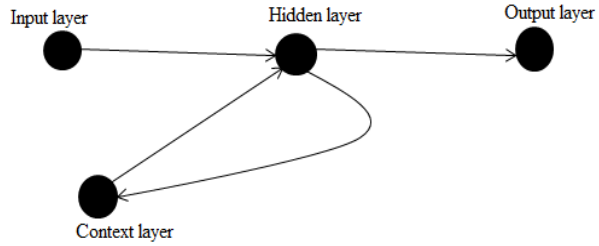

Figure 2: The Elman network (Kröse and van der Smagt, 1996)

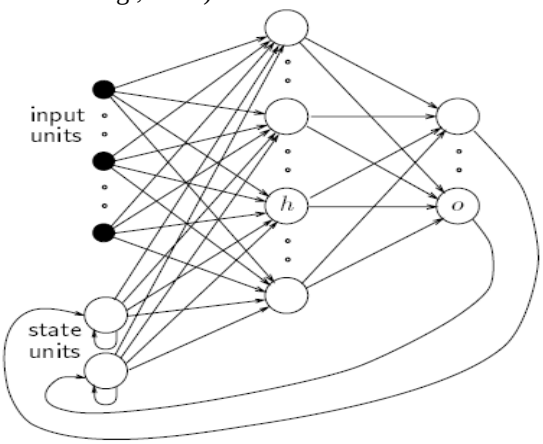

Figure 3: The Jordan network (Kröse and van der Smagt, 1996)

However, many real-world problems are solved when feed forward network topologies are used instead of recurrent networks, which are more difficult to employ (Pearlmutter, 1990).

Artificial neural networks training

The construction of a neural network should be done in such a way that when a set of inputs is applied, the desired set of outputs is produced. This is accomplished by either clearly setting the weights based on a priori knowledge, or by training the machine by feeding it teaching configurations and

allowing it to adjust its weights based on some learning instructions.

There are two types of learning in neural networks: supervised (associative) learning and unsupervised learning (self-organization).

Supervised (associative) learning is a sort of learning in which the network is changed based on output and target comparisons until the network output matches the target. An external trainer or the system containing the network (self-supervised) can offer these input-output pairings (Demuth and Beale, 2002; Kröse and van der Smagt, 1996).

Unsupervised (self-organization) learning, on the other hand, is a sort of learning in which an output is trained to respond to collections of patterns within the input by identifying statistically significant aspects of the population. The system creates its own representation of the incoming stimuli in this sort of learning, and there is no predetermined set of categories into which the patterns should be classified (Demuth and Beale, 2002; Haykin, 2001).

Multi-layer feed-forward networks

A neural network connection can be either a single-layer connection with significant constraints on the types of activities that can be done, or a multi-layer connection with more flexibility (Graupe, 2007; Hu and Hwang, 2002).

To determine the network parameters, a variety of algorithms are used. In the field of neural networks, the algorithms are known as learning or teaching algorithms (Poulton, 2001). Back-propagation and Levenberg-Marquardt algorithms are two of the most well-known algorithms. Back-propagation learning rule was first proposed by Rumelhart, Hinton, and Williams in 1986 (Rumelhart *et al*., 1986), where the errors for the hidden layer units are determined by back-propagating the errors of the output layer units. This is a gradient-based algorithm with a lot of variations. The Levenberg-Marquardt approach, on the other hand, is more efficient than back propagation since it saves time (Bishop, 1995; Haykin, 2001; Poulton, 2001).

Artificial Neuron's Major Components

This section describes the major components of the artificial neuron using information from a variety of sources, including (Anderson and McNeill, 1992; Anderson, 1997; Demuth and Beale, 2002; Galushkin, 2007; Haykin, 2001).

The weighting factors are the first component. Weights are network adaptable coefficients that control the strength of the input signal as perceived by the artificial neuron. They are numerical elements that connect the output value of a neuron to the next neuron to which it is connected. They are also a measure of an input's connection strength, which might change in response to different training sets, as well as a network's structure and learning rules.

Summation function is the second component in which, if the inputs and weights are vectors that can be represented as $X = [x_1, x_2... x_n]^T$ and $W = (w_1, w_2... w_n)$, then, the summing function is calculated by

multiplying each component of the X vector by the corresponding component of the W vector and then adding up all the products. Thus:

$$X^T.W = x_1w_1 + x_2w_2 + ...+ x_nw_n = \sum_{i=1}^{n} x_iw_i \quad (9)$$

This summation must be passed on to the transfer or activation function for the summation result to vary with time.

In the third component, when the product of the inputs and weights is obtained, the result is turned into the output via an algorithmic process known as the transfer function, which is often non-linear. The hyberbolic tangent (tanh) and a sigmoid function are the most widely employed activation functions.
Scaling and limiting make up the fourth component. This is a procedure in which the outcome of the transfer function of the processing element passes through. It simply adds an offset after multiplying a scaling factor by the transfer value. Its core function is to make sure the scaled result doesn't go beyond a certain limit. This limiting is also in addition to any limitations imposed by the initial transfer function.

In the fifth component, output function (competition), one output signal from each processing unit passes to hundreds of additional neurons. In most cases, the network's output is identical to the transfer function's output. During the process, some network topologies' transfer outcomes may be adjusted to accommodate competition among neighboring processing nodes. Neurons can compete against one another in this process. The competition's goal is to figure out which artificial neuron will be active in generating an output or which processing unit will be involved in the learning or adaption process.

The error function and back-propagated value make up the sixth component. The obtained output always differs from the targeted output during the process of determining the output, and the difference is calculated. The error function then adjusts the error between these two outputs to reflect the network design. Most basic neural network topologies employ this error directly; however, some of them square the error while keeping its sign, while others adjust the raw error to serve their special needs. The error of the generated artificial neuron is then propagated backwards to a previous layer by being sent through the learning function of another processing element. After the learning function has scaled this back-propagated value, it is multiplied against each of the incoming connection weights in order to change them before the next learning cycle.

The learning function is the final component, and it is used to adjust the weights of the input connections in order to obtain certain outputs. This function is also known as the adaption function or the learning mode, and it is used to change the variable connection weights on the inputs of each processing unit using a neural-based algorithm.

Single-node multilayer perceptron

Figure 5 depicts a multilayer perceptron (MLP) network.

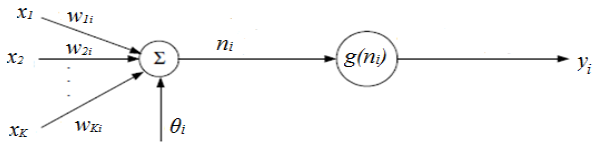

Figure 4: An example of a single node in a MLP network (Demuth and Beale, 2002)

To obtain the output $y = n_i$, the inputs x_k, $k = 1, 2, ...K$ to the neuron are multiplied by weights and added together with the constant bias factor θ_i.

$$y = n_i = \sum_{j=1}^{K} w_{ji} x_j + \theta_i \qquad (10)$$

The resulting n_i is used as an input to the activation function $g_i = g(n_i)$, and the final output is as follows:

$$y_i = g_i = g\left(\sum_{j=1}^{K} w_{ji} x_j + \theta_i\right) \qquad (11)$$

Multilayer Perceptron with more than one node

Figure 6 depicts an MLP network generated when many nodes are joined in parallel and series. The activation function g has been employed in both layers, as shown in the Figure 6, and the superscripts in *θ, n*, or *w* specifies the network layer. The equation for the final output in Figure 6 can be determined by considering the expression for the output value given in equation (11).

The first inputs and weights produce the following output:

$$g_i = g\left(n_j^1\right) = g\left(\sum_{k=1}^{K} w_{kj}^1 x_k + \theta_j^1\right) \qquad (12)$$

The final output y_i, i = 1, 2, can now be given as;

$$y_i = g\left(\sum_{j=1}^{3} w_{ji}^2 g\left(n_j^i\right) + \theta_j^2\right) = g\left(\sum_{j=1}^{3} w_{ji}^2 g\left(\sum_{k=1}^{K} w_{kj}^1 x_k + \theta_j^1\right) + \theta_j^2\right) \qquad (13)$$

.

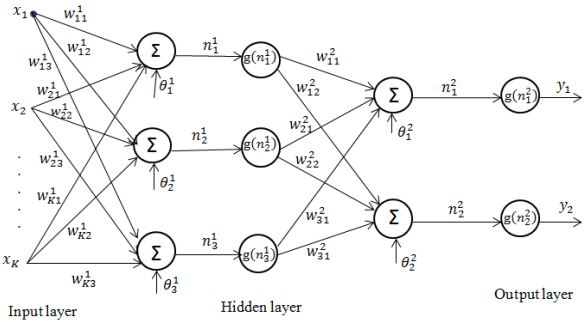

Figure 5: A multilayer perceptron network with one hidden layer

When using a set of training samples that include input values x^p and desired (or target) output values d^p, where p is the number of iterations, the network's output is always different from the target value. If y^p is the network's actual output, then d^p - y^p is the difference between it and its target output. The weights are changed based on these differences in order to achieve the best output values (Kröse and van der Smagt, 1996).

The error function (least mean square error) is calculated using the summed squared error E given as;

$$E = \sum_p E^p = \frac{1}{2}\sum_p \left(d^p - y^p\right)^2 \qquad (14)$$

where the index p ranges over the set of input patterns and E^p represents the error on pattern p.

The Least-Mean-Square (LMS) approach is used to find the values of all the weights using a method called gradient descent in order to minimize the error function. A weight change is proportional to the negative of the derivative of the error

measured on the current pattern with respect to each weight (Kröse and van der Smagt, 1996).

$$\Delta_p w_j = -\gamma \frac{\partial E^p}{\partial w_j} \tag{15}$$

Where γ is the learning-rate parameter, which is a proportionality constant. To reduce the value of E^p, the minus sign in equation (15) accounts for gradient descent in weight space. Equation (15) can be rearranged to give the following result:

$$\frac{\partial E^p}{\partial w_j} = \frac{\partial E^p}{\partial y^p}\frac{\partial y^p}{\partial w_j} \tag{16}$$

From equation (10),

$$\frac{\partial y^p}{\partial w^p} = x_j \tag{17}$$

and from (14),

$$\frac{\partial E^p}{\partial y^p} = -\left(d^p - y^p\right) \tag{18}$$

Thus,

$$\Delta_p w_j = \gamma \delta^p x_j . \tag{19}$$

where $\delta^p = d^p - y^p$

Based on this relationship, the weight can be adjusted suitably for target and actual outputs of either polarity for input and output units of the network.

Early stopping training approach

The mean square error diminishes as the number of epochs increases in the back-propagation process. This is due to the fact that, the multilayer perceptron learns in phases, ranging from simple to more complicated functions throughout the training session. If the training session is not interrupted at the proper point, the network may end up overfitting the training data. To circumvent this, the training data is divided into two parts: estimation (training) and validation (validation). The network is trained using the estimation part of the data and paused every now and then, and the validation part of the data is utilized to test the data after each training session. The estimation session is restarted for another period when the validation procedure is completed; the process is repeated until the optimal value is achieved (Demuth and Beale, 2002; Haykin, 2001).

Studies based on Neural Networks approach

Neural networks (NNs) are powerful predictive modeling tools that combine machine learning and pattern recognition capabilities. They can recognize patterns and trends in specific data and, as a result, correctly anticipate future trends and patterns in the data. Demuth and Beale (2002) and Okoh *et al*. (2016) demonstrated that a neural network may be trained to execute a certain purpose by altering the weights. The capacity of neural networks to capture both linear and nonlinear relationships directly from the data being modeled is one of its most powerful features (Okoh *et al*., 2016).

The capability of neural networks in ionospheric modeling has been proved in a number of researches conducted in various locations. According to Okoh *et al*., (2016) in their study on a regional GNSS-TECv model over Nigeria utilizing neural networks, DST, SSN, and IRI-foF2 as input

layer neurons on the networks are effective in boosting the network performances. They implemented Levenberge-Marquardt backpropagation algorithm because of its speed and efficiency in learning. When comparing TEC predictions from the NN with the IRI model, Okoh et al. (2016) observed that, the developed model makes better predictions than the IRI model. Habarulema *et al*. (2007) used a feed forward network with back propagation algorithm and found that NNs are suitable for forecasting GPS TEC values at places inside South Africa, and that their results were able to predict the TEC values more correctly than IRI-2001. They also demonstrated that the NN model accurately forecasts the trend of GPS TEC diurnally and seasonally, while the created model overestimates or underestimates the TEC in some cases. The same study indicated that correlation coefficients between the NN modeled TEC and GPS TEC were more consistent as compared to those from the IRI-2001 model over South African region. When the verification data set used is within the training data set range, the NN based model's prediction accuracy is more apparent (Habarulema *et al*., 2011).

Homam (2014) discovered that a network configuration that uses TEC values during lower solar activity had a lower Root-Mean Square Error (RMSE), as well as absolute and relative error, than a network configuration that uses TEC values during higher solar activity. Homan chose to use Levenberg-Marquardt back propagation algorithm due to its fast processing, although it needs more memory when compared with other algorithms. Leandro and Santos (2007) used the Levenberg-Marquardt back-propagation algorithm to train the neural network model for regional vertical total electron content simulation utilizing the Brazilian network data. The findings revealed that the neural network model gave TEC value approximations with an average absolute error of 3.7 TECU and a standard deviation of 2.7 TECU.

Sulungu and Uiso (2019) established a model for GPS TEC prediction across Eastern Africa using a neural network (NN) approach. They used the multi-layer perceptron neural network because of its speed and efficiency during learning process. According to their findings, the more input layer neurons that were added to the networks, the better the networks learned and produced the improved results. They also found that when sunspot numbers (SSN) and the IRI-NmF2 were incorporated as input neurons, correlation coefficients indicated that, the created NN model could accurately predict GPS TEC. Sulungu and Uiso (2019) also found that the generated NN model well predicted the diurnal variational pattern of the TEC parameter, and that the model closely matched the GPS TEC in most cases when compared to the IRI-2012 model. This result was also obtained by Sahu *et al*. (2021) on their study on prediction of TEC using NN, utilizing the Levenberg-Marquardt algorithm, over anomaly crest region Bhopal.

Okoh *et al*. (2020) used a neural network approach to create a storm-time total electron content (TEC) model over the

African sector. They trained the network using Bayesian regularization backpropagation algorithm. In comparison to low and equatorial latitude regions, the model performed better in mid-latitude. Sivavaraprasad *et al*. (2020) studied the performance of TEC forecasting models based on Neural Networks (NN) across equatorial low latitude Bengaluru, India. They used Levenberg-Marquardt algorithm as the training technique due to its speed and efficiency in learning and found that the NN model was more accurate than IRI-2016 model. Y By using Bayesian Regularization process according to Levenberg-Marquardt optimization, Cesaroni *et al*. (2020) forecasted Total Electron Content (TEC) 24 hours ahead of time at a global scale. They obtained a very satisfactory result in terms of RMSE, ranging between 3 and 5 TECU.

Tulunay *et al*. (2004) utilized the Levenberg-Marquardt backpropagation algorithm in training the Middle East Technical University Neural Network based models, to estimate 10-minute TEC variations during the high solar activity of 2000-2001, and the NN model's sensitivity and accuracy were found to be good. They concluded that the methodologies they developed can be utilized to characterize the electromagnetic wave propagation medium for the purposes of planning and operation of radio systems. Watthanasangmechai *et al*. (2012) applied the Levenberg-Marquardt algorithm as the training function in their investigations on TEC prediction with neural networks for equatorial latitude stations in Thailand. Their results showed a good prediction of TEC by the NN model compared to the IRI-2007 model. Their findings also demonstrated that, large variations in TEC made it hard for the NN to learn during specific periods, and they linked this problem to the formation of an equatorial plasma bubble as well as day-to-day TEC variations in the equatorial area. When Uwamahoro and Habarulema (2015) were modeling total electron content during geomagnetic storm conditions in South Africa, they trained the network using the Leverberg-Marquardt back propagation algorithm because of its time saving advantage during training and found that the choice of hidden node number could alter the NN prediction capability.

Li and Wu (2023) developed an Ionospheric TEC Model with a storm option over Japan based on a multi-layer perceptron (MLP) neural network. The maximum RMSE was lower than 2TECU, while the corresponding RMSEs for the IRI exceeded 5TECU. Shenvi and Virani (2023) forecasted the ionospheric TEC using a multivariate deep long short-term memory (LSTM) model for different latitudes and solar activity. Their results showed that, LSTM predicted TEC with more accuracy than MLP. MLPs fail to predict accurately in cases where the data is noisy or turbulent, particularly during solar active years and during the occurrence of geomagnetic. Smirnov et al (2023) developed a neural network-based model of electron density in the topside ionosphere, and shows outstanding agreement with the observations, beating the IRI model, especially at 100-200 km above the F2-layer peak. An artificial neural network model developed by Ozkan (2022), based on

Levenberg-Marquardt backpropagation algorithm, for predicting VTEC over central Anatolia in Turkey, showed better performance than the global IRI-2016 model. Adolfs and Hoque (2021) established a neural network-based TEC model capable of reproducing nighttime winter anomaly. NN model results were compared with the Neustrelitz TEC Model (NTCM), and the results showed that, the neural network model outperformed the NTCM by approximately 1 TECU. Okoh et al. (2019) developed a neural network-based ionospheric model over Africa from constellation observing system by training the networks using the Bayesian regularization back-propagation algorithm. After testing the usefulness of three solar activity indices (sunspot number, solar radio flux at 10.7-cm wavelength [F10.7], and solar ultraviolet [UV] flux at 1 AU), the F10.7 and UV were more operative, and the F10.7 was chosen since it produced the smallest errors on the validation data set used.

Several studies (Conway *et al*., 1998; Habarulema *et al*., 2007; Maruyama, 2009; Okoh *et al*., 2016; Watthanasangmechai *et al*., 2012) shown that, the NN model performs well when data is collected over a long period of time, at least one solar cycle (11 years). However, investigations by Leandro and Santos (2007) and Homam (2014) found that, the NN model can accurately predict GPS TEC even with data from shorter time periods. Therefore, from this survey of literature, it shows that, Levenberg-Marquardt algorithm is preferred and used mostly because of its speed and efficiency during learning process. It is also found that NN is able to forecast TEC values more correctly than the IRI model.

CONCLUSION

According to the literature survey, building a neural network should be done in such a way that, applying a set of inputs results in the desired set of outputs. This is accomplished by either clearly setting the weights based on a priori knowledge, or by training the machine by feeding it teaching configurations and allowing it to adjust its weights based on some learning instructions. The survey from literature reveals that, Levenberg-Marquardt algorithm is preferred and used mostly because of its speed and efficiency during learning process. It is also found that NN is able to forecast TEC values more correctly than the IRI model, as well as the trend of GPS TEC diurnally and seasonally, although the model over or underestimates the TEC in some cases. It is also clear that the number of hidden nodes chosen can have an impact on the NN's capacity to forecast. The research also has shown that, the NN model performs well when data is collected over lengthy periods of time, at least one solar cycle (11 years), while some investigations revealed that the NN model can predict GPS TEC even with data collected over shorter time periods.

Therefore, the Levenberg-Marquardt algorithm is a popular optimization technique used for training artificial neural networks. It is an efficient method for minimizing non-linear least squares problems and is often employed for training

neural networks due to its fast convergence properties.

However, after going through different literature on application of NN in predicting TEC, the following recommendations are made for future research:

Investigation on the incorporation of temporal and spatial features to capture the dynamic nature of the Earth's ionosphere should be done. ANNs capable of processing spatiotemporal data might yield more accurate predictions.

Exploring the potential of transfer of learning is essential, where knowledge learned from one region or dataset is transferred to improve predictions in another region with limited data.

Investigation of techniques to adapt ANNs trained on data from one geographical location to be effective in different but related regions.

ACKNOWLEDGEMENT

I wish to acknowledge all members of Physics department, University of Dodoma, for their supportive comments and ideas towards successful writing of this article.

REFERENCES

Adewale, A. O., Oyeyemi, E. O., Adeniyi, J. O., Adeloye, A. B., and Oladipo, O. A. (2011). Comparison of total eletcron content predicted using the IRI-2007 model with GPS observations over lagos, Nigeria. *Indian J. Radio and Space Ph*. 40, 21-25.

Adolfs, M., Hoque, M. M. (2021). A Neural Network-Based TEC Model Capable of Reproducing Nighttime Winter Anomaly. *Remote Sens*. 13, 4559. https://doi.org/10.3390/rs13224559.

Akir, R. M., Abdullah, M., Chellappan, K., and Hasbi, A. M. (2015). Preliminary Vertical TEC Prediction Using Neural Network: Input Data Selection and Preparation. Proceeding of the 2015 *International Conference on Space Science and Communication (Icon Space),* 10-12 August 2015, Langkawi, Malaysia.

Anderson, D., and McNeill, G. (1992). Artificial Neural Networks Technology. Kaman Sciences Corporation, New York.

Anderson, J. A. (1997). An introduction to neural networks. Massachusetts Institute of Technology, Massachusetts, USA.

Bhuyan, P. K., and Borah, R. R. (2007). TEC derived from GPS network in India and comparison with the IRI. *Adv. Space Res*. 39(5):830–840.

Bilitza, D. (1986). International reference ionosphere: recent developments. *Radio Sci*. 21: 343–346.

Bilitza, D., Altadill, D., Zhang, Y., Mertens, C., Truhlik, V., Richards, P., McKinnell, L., and Reinisch, B. (2014). The International Reference Ionosphere 2012 – a Model of International collaboration. *J. Space Weather Space Clim*. 4: A07.

Bilitza, D., and Reinisch, B. W. (2008). International Reference Ionosphere 2007: Improvements and new

parameters. *Adv. Space Res*. 42: 599–609.

Bishop, C. (1995). Neural Networks for Pattern Recognition. Oxford Press, Oxford.

Cesaroni, C., Spogli, L., Aragon-Angel, A., Fiocca, M., Dear, V., De Franceschi, G., and Romano, V. (2020). Neural network-based model for global Total Electron Content forecasting. *J. Space Weather Space Clim*. 10, 11. https://doi.org/10.1051/swsc/2020013

Chauhan, V., Singh, O. P., and Singh, B. (2011). Diurnal and Seasonal variation of GPS-TEC during a low solar activity period as observed at a low latitude station Agra. *Indian J. Radio and Space Ph.* 40 (1): 26–36.

Chen, Z., Liao, W., Li, H., Wang, J., Deng, X., and Hong, S. (2022). Prediction of global ionospheric TEC based on deep learning. *Space Weather*, 20, e2021SW00285. https://doi.org/10.1029/2021SW002854.

Conway, A. J., Macpherson, K. P., Blacklaw, G., and Brown, J. C. (1998). A neural network prediction of solar cycle 23. J. *Geophys. Res*. 103: 29,733-29,742.

Demuth, H., and Beale, M. (2002). Neural Network Toolbox for Use with MATLAB. User's Guide Version 4. The MathWorks, Inc. Natick, USA.

Eddy, J. A. (2009). The Sun, the Earth, and near-Earth Space: Guide to the Sun-Earth system. National Aeronautics and Space Administration (NASA), Washington.

Galushkin, A. I. (2007). Neural Networks Theory. Springer-Verlag Berlin, Heidelberg.

Gao, Y., and Liu, Z. Z. (2002). Precise ionosphere modeling using regional GPS network data. *J. Global Pos. Systems*. 1(1): 18-24.

Graupe, D. (2007). Principles of Artificial Neural Networks, 2nd Edition. Advanced Series on Circuits and Systems, Vol. 6. World Scientific Publishing Co. Pte. Ltd. Singapore.

Guoyan, L., Wang, G., Zhengxie, Z., and Qing Z., (2021). Prediction of Ionospheric TEC Based on the NARX Neural Network. *Hindawi, Mathematical Problems in Engineering*, ID 7188771, 1 – 10. https://doi.org/10.1155/2021/7188771

Habarulema, J. B. (2010). A contribution to TEC modeling over Southern Africa using GPS data. PhD Thesis, University of Rhodes.

Habarulema, J. B., McKinnell, A., Opperman, and B. D. L. (2011). Regional GPS TEC modeling; Attempted spatial and temporal extrapolation of TEC using neural networks. *J. Geophys. Res: Atmospheres*. 116: A04314.

Habarulema, J. B., McKinnell, L., and Cilliers, P. J. (2007). Prediction of global positioning system total electron content using Neural Networks over South Africa. *J. Atmos. Sol. Terr. Phys*. 69: 1842–1850.

Hanslmeier, A. (2002). The Sun and Space Weather. Astrophysics and Space Science Library Vol. 277. Kluwer Academic Publishers, Dordrecht.

Haykin, S. (2001). Neural Networks: A Comprehensive Foundation. Second Edition. Pearson Education (Singapore) Pte. Ltd, Indian branch, Delhi.

Homam, M. J. (2014). Initial Prediction of Total Electron Content (TEC) At a Low Latitude Station Using Neural Network. *2014 IEEE Asia-Pacific Conference on Applied Electromagnetics*, 8 – 10 December 2014 at Jonor Bahru, Malaysia.

Hu, Y. H., and Hwang, J. N. (2002). Handbook of Neural Network Signal Processing. CRC press, Florida.

Hunt, S. M., Close, S., Coster, A. J., Stevens, E., Schuett, L. M., and Vardaro, A. (2000). Equatorial atmospheric and ionospheric modeling at Kwajalein missile range. *Lincoln Lab. Journal*. 12 (1): 45-64.

Kataoka, R., and Pulkkinen, A. (2008). Geomagnetically Induced Currents during intense storms driven by coronal mass ejections and corotating interacting regions. *J. Geophys. Res*. 113: A03S12.

Kelley, M. C. (2009). The Earth's Ionosphere Plasma Physics and Electrodynamics, Second Edition. Academic Press, London.

Kenpankho, P., Watthanasangmechai, K., Supnithi, P., Tsugawa, T., and Maruyama, T. (2011). Comparison of GPS TEC measurements with IRI TEC prediction at the equatorial latitude station, Chumphon, Thailand. *Earth, Planets and Space* 63: 365–370.

Kröse, B., and van der Smagt, P. (1996). An Introduction to Neural Networks. Eighth edition. The University of Amsterdam, Amsterdam.

Kumar, K., Leong, T., and Murti, D. S. (2015). Impacts of solar activity on performance of the IRI-2012 model predictions from low to mid-latitudes. *Earth, Planets and Space*. 67:42, DOI 10.1186/s40623-015-0205-3.

Leandro, R. F., and Santos, M. C. (2007). A Neural Network Approach for Regional Vertical Total Electron Content Modelling. Stud. *Geophys. Geod*. 51: 279-292.

Lee, S., Ji, E. Y., Moon, Y. J., and Park, E. (2021). One-day forecasting of global TEC using a novel deep learning model. *Space Weather*, 19, e2020SW002600. https://doi.org/10.1029/2020SW002600.

Leitinger, R., Nava, B., Hochegger, G. and Radicella, S. (2001). Ionospheric profilers using data grids. Physics and Chemistry of the Earth, Part C. *Solar, Terrestrial & Planetary Science* 26: 293–301.

Leong, S. K., Musa, T. A. and Abdullah, K. A. (2011). Spatial and temporal variations of GPS-Derived TEC over Malaysia from 2003 to 2009. *ISG & ISPRS 2011*, Sept. 27-29, 2011 – Shah Alam.

Li, W., Wu, X. (2023). An Ionospheric Total Electron Content Model with a Storm Option over Japan Based on a Multi-Layer Perceptron Neural Network. *Atmosphere*, 14, 634.

https://doi.org/10.3390/atmos14040634.

Liu, G., Huang, W., Gong, J., and Shen, H. (2013). Seasonal variability of GPS-VTEC and model during low solar activity period (2006–2007) near the equatorial ionization anomaly crest location in Chinese zone. *Adv. Space Res*. 51:366–376.

Maruyama, T. (2009). Regional Reference Total Electron Content Model over Japan Using Solar EUV Proxies. *J. National Inst. Info. and Communic. Techn*. 56 (4): 407 – 424.

Memarzadeh,Y. (2009). Ionospheric modeling for precise GNSS applications. PhD thesis, Delft Institute of Earth observation and Space systems (DEOS), Delft University of Technology.

Nigussie, M., Radicella, S. M., Damtie, B., Nava, B., Yizengaw, E., and Ciraolo, L. (2012). TEC ingestion into NeQuick 2 to model the East African equatorial ionosphere. *Radio Sci*. 47 (5): RS5002.

Norsuzila, Y., Abdullah, M., and Ismail, M. (2010b). GPS Total Electron Content (TEC) prediction at ionosphere layer over the equatorial region. In: Bouras CJ (ed) Trends in Telecommunications Technologies, In Tech, Rijeka.

Norsuzila, Y., Abdullah, M., Ismail, M., Ibrahim, M., and Zakaria, Z. (2010a). Total Electron Content (TEC) and estimation of positioning error using Malaysia data. *Proceedings of the world congress on Engineering* Vol. I, June 30 - July 2, 2010, London.

Okoh, D., Habarulema, J. B., Rabiu, B., Seemala, G., Wisdom, J. B., Olwendo, O., Obrou, O., and Matamba, T. M. (2020). Storm-Time Modeling of the African Regional Ionospheric Total Electron Content Using Artificial Neural Networks. *Space Weather*. 18, e2020SW002525. https://doi.org/10.1029/2020SW002525

Okoh, D., Owolabi, O., Ekechukwu, C., Folarin, O., Arhiwo, G., Agbo, J., Bolaji, S., and Rabiu, B. (2016). A regional GNSS-VTEC model over Nigeria using neural networks: A novel approach. *Geod. and Geodyn*. 17 (1): 19 -31.

Okoh, D., Seemala, G., Rabiu, B., Habarulema, J. B., Jin, S., Shiokawa, K., et al. (2019). A neural network-based ionospheric model over Africa from Constellation Observing System for Meteorology, Ionosphere, and Climate and Ground Global Positioning System observations. *Journal of Geophysical Research*: *Space Physics*, 124. https://doi.org/10.1029/2019JA027065

Oron, S., D'ujanga, F. M., and Ssenyonga, T. J. (2013). Ionospheric TEC variations during the ascending solar activity phase at an equatorial station, Uganda. *Indian J. Radio and Space Phys*. 42 (1):7–17.

Ozkan, A. (2022). An artificial neural network model in predicting VTEC over central Anatolia in Turkey. *Geodesy and Geodynamics* 14. 130 - 142.

Pearlmutter, B. A. (1990). Dynamic Recurrent Neural Networks. Technical Report No. CMU – CS – 90 – 196. Pittsburgh, PA 15213: School of Computer Science, Carnegie Mellon University.

Poulton, M. M. (2001). Computational Neural Networks for Geophysical Data Processing. Pergamon, Oxford.

Rathore, V. S., Kumar, S., and Singh, A. K. (2015). A statistical comparison of IRI TEC prediction with GPS TEC measurement over Varanasi. *J. Atmos. Sol. Terr. Phys*. 124: 1–9.

Rumelhart, D., Hinton, G., and Williams, R. (1986). Learning representations by error propagation. In: Rumelhart DE and McClelland JL (ed). Parallel Distributed Processing. MIT Press, Massachusetts.

Sahu, S., Trivedi, R., Choudhary, R. K., Jain, A., and Jain, S. (2021). Prediction of Total Electron Content (TEC) using Neural Network over Anomaly Crest Region Bhopal, *Advances in Space Research*. https://doi.org/10.1016/j.asr.2021.05.027

Shenvi, N., and Virani, H. (2023). Forecasting of Ionospheric Total Electron Content Data Using Multivariate Deep LSTM Model for Different Latitudes and Solar Activity. *Journal of Electr. and Computer Engin.* 2855762, https://doi.org/10.1155/2023/2855762.

Shim, J. S. (2009). Analysis of Total Electron Content (TEC) variations in the low and middle latitude ionosphere. PhD Thesis, Department of Physics, Utah State University.

Sivavaraprasad, G., Deepika, V. S., SreenivasaRao, D., Ravi Kumar, M., and Sridhar, M. (2020). Performance evaluation of neural network TEC forecasting models over equatorial low-latitude Indian GNSS station. *Geodesy and Geodynamics*. 11: 192 – 201.

Smirnov, A., Shprits, Y., Prol, F., Lühr H., Berrendorf, M., Zhelavskaya, I., and Xiong C. (2023). A novel neural network model of Earth's topside ionosphere. *Scientific Reports* 13:1303 https://doi.org/10.1038/s41598-023-28034-z.

Sulungu, E. D., and Uiso, C. B. S. (2019). Total Electron Content Prediction Model using the Artificial Neural Networks over the Eastern Africa Region. *Tanz. J. Sci*. 45(3): 502-517.

Sulungu, E. D., Uiso, C. B. S., and Sibanda, P. (2018a). Comparison of GPS derived TEC with the TEC predicted by IRI 2012 model in the southern Equatorial Ionization Anomaly crest within the Eastern Africa region. *Advances in Space Research*. 61: 1660–1671.

Sulungu, E. D., Uiso, C. B. S., and Sibanda, P. (2018b). Total Electron Content Derived from Global Positioning System During Solar Maximum of 2012-2013 Over the Eastern Part of the African Sector. *Tanz. J. Sci*. 44(1): 62-74.

Tang, J., Li, Y., Ding, M., Liu, H., Yang, D., and Wu, X. (2022). An Ionospheric TEC Forecasting Model Based on a

CNN-LSTM-Attention Mechanism Neural Network. *Remote Sens*. 14, 2433. https://doi.org/10.3390/rs14102433.

Tulunay, E., Senalp, E. T., Cander, L. R., Tulunay, Y. K., Bilge, A. H., Mizrahi, E., Kouris, S. S. and Jakowski, N. (2004). Development of algorithms and software for forecasting, nowcasting and variability of TEC. *Ann. Geophys*. 47 (2): 1201 – 1214.

Unnikrishnana, K., Haridasb, S., Choudharyc, R. K., and Bosed, P. D. (2018). Neural Network Model for the Prediction of TEC Variabilities over Indian Equatorial Sector. *Indian J. Sci. Res*. 18(1): 56 – 58

Uwamahoro, J. C., and Habarulema, J. B. (2015). Modelling total electron content during geomagnetic storm conditions using empirical orthogonal functions and neural networks, *J. Geophys. Res. Space Physics* 120: 11,000–11,012.

Watthanasangmechai, K., Supnithi, P., Lerkvaranyu, S., Tsugawa, T., Nagatsuma, T., and Maruyama, T. (2012). TEC prediction with neural network for equatorial latitude station in Thailand. *Earth, Planets and Space* 64: 473–483.

Wik, M., Pirjola, R., Lundstedt, H., Viljanen, A., Wintoft, P., and Pulkkinen, A. (2009). Space Weather events in July 1982 and October 2003 and the effects of Geomagnetically Induced Currents on Swedish technical systems. *Ann. Geophys*. 27: 1775–1787.

Xiong, P., Zhai, D., Long, C., Zhou, H., Zhang, X., and Shen, X. (2021). Long short-term memory neural network for ionospheric total electron content forecasting over China. *Space Weather*, 19, e2020SW002706. https://doi.org/10.1029/2020SW002706.